# Modeling the Performance of Ionic Liquid-Water Mixtures in an Air Conditioning Application

Abdulaziz El-Sinawi[1], Karthik Silaipillayarputhur[1*], Christopher Hardacre[2],
Saad Al-Mubarak[1], Mohammed Abdulmohsen Almuhaysh[1]

[1]*King Faisal University, KINGDOM of SAUDI ARABIA.*
[2]*The University of Manchester, UNITED KINGDOM.*
*Corresponding Author (Email: ksilai@kfu.edu.sa).*

## Abstract

This research examines the design of an air conditioning process. The various steps in the air conditioning process are described. A range of air conditioning layouts, mixing proportion of fresh air with re-circulated air, human comfort settings, and estimating the best supply condition is described in the paper. Comfort air conditioning is established based on accepted engineering standards from ASHRAE (The American Society of Heating, Refrigerating and Air-Conditioning Engineers). The cooling coil, an integral part of an air conditioning system, is a finned cross-flow heat exchanger. The design of the cooling coil is modeled using various secondary refrigerants, conventional chilled water and ionic liquid-water mixtures. The use of ionic liquid-water mixtures as secondary refrigerants in an air conditioning process is a new concept. The use of ionic liquid-water mixtures as heat transfer fluid in sensible heating and cooling applications has been studied due to the ionic liquid's physical characteristics such as chemical and thermal stability, non-volatility, tunable solubility in water, etc. In this work, four different kinds of ionic liquid-water mixtures are considered secondary refrigerants for the cooling coil. The design of the cooling coil is considered on a dimensionless basis, and the parameters relevant to steady-state heat exchanger modeling are applied. For the given operating conditions and cooling load, both chilled water and ionic liquid-water mixtures required a similar number of transfer units (NTU) for achieving the desired heat transfer.

**Disciplinary:** Mechanical Engineering.

**©2022 INT TRANS J ENG MANAG SCI TECH.**

# 1 Introduction

This paper consists of two parts. In the first half of the manuscript, the detailed air conditioning design of a mechanical engineering lab at King Faisal University is presented. Therein, the heating load in the mechanical engineering lab is first evaluated. The human comfort conditions are established using ASHRAE engineering standards. Different air conditioning layouts and mixing proportions are considered therein. The air conditioning design is established such that the required project constraints are addressed. In the second half of the manuscript, the cooling coil design for the air conditioning process is compared using chilled water and ionic liquid-water mixtures. The cooling coil is a finned cross-flow heat exchanger and the design of the cooling coil is established in terms of dimensionless parameters. These parameters govern the steady state performance of a heat exchanger. For brevity, only the design of the air conditioning process and the design of the cooling coil (air-to-coolant cross-flow heat exchanger) are shown in this paper.

Ionic liquid-water mixtures are gaining popularity due to their inherent characteristics such as chemical and thermal stability, energy storage, low freezing point, low vapor pressure, etc. The paper evaluates the performance of ionic liquid-water mixtures as a secondary refrigerant. In this project, a comparative study on various coolants such as chilled water, ionic liquid mixtures with $H_2O$ composed of the tetradecyl trihexyl phosphonium ($[P_{14,6,6,6}]^+$) cation coupled with butanoate ($[ButO]^-$: $C_3H_7COO^-$), hexanoate ($[HexO]^-$: $C_5H_{11}COO^-$), octanoate ($[OctO]^-$: $n\text{-}C_7H_{15}COO^-$), and decanoate ($[DecO]^-$: $n\text{-}C_9H_{19}COO^-$) anions have been studied. It must be noted that the properties of ionic liquid-water mixtures can be readily altered by adjusting the concentration of water and by altering the chemical structure of anion and cation. For favorable pumping, and for favorable convection heat transfer, various thermo physical properties such as dynamic viscosity, density, thermal conductivity, specific heat, etc. are of significance. Based on the application, the properties of ionic liquid-water mixtures can be quickly altered according to the requirements.

The ionic liquid-water mixtures have been studied for refrigeration applications. Specifically, they have been widely considered in the absorption refrigeration system. However, the application of ionic liquid-water mixtures is not yet widely considered (as a secondary refrigerant) in the conventional vapor compression refrigeration system.

Oster et al. (2018) described the production of ionic liquid-water mixtures and their thermo physical properties. Oster et al. (2018) also reported various models for predicting the thermal properties of pure ionic liquids, in particular, their thermal conductivity and heat capacity. Chereches and Minea (2021) experimentally evaluated the electrical conductivity of ionic liquid-water mixtures and alumina nanoparticles. Nimmagadda et al. (2021) numerically investigated the thermal performance of unidirectional and bidirectional lid-driven cavities using ionic liquids enhanced with nanoparticles. Prasher et al. (2021) studied the use of ionic liquids in photonic heaters used in solar desalination. El Sinawi et al. (2021) investigated the performance of ionic liquid-water mixtures in an acetone cooling application using a double pipe heat exchanger. Chereches et al. 2019 experimentally investigated the thermo-physical properties of ionic liquids

enhanced with nanoparticles. Asensio-Delgado et al. (2021) examined the absorption separation of refrigerant vapor with ionic liquids. Ferwati et al. (2021) studied ionic liquid-water mixtures as an alternative refrigerant for the absorption refrigeration system. Varela et al. 2020 examined ionic liquids via experimentation and simulation for a desiccant air conditioning system. Watanabe et al. 2019 also reported the use of ionic liquids as liquid desiccants for air conditioning systems. Silaipillayarputhur and Idem (2013) developed a procedure to understand the steady state performance of cross-flow heat exchangers. Zhai et al. (2021) considered an absorption refrigeration system using water and ionic liquids. Therein, they employed plate heat exchangers as absorbers in the absorption refrigeration system. Liu et al. 2022 considered the working pairs of dimethyl ether and ionic liquids for absorption refrigeration systems. The solubility of dimethyl ether with ionic liquids was measured. The combinations presented in the work yield high COP, and have environmental friendliness. Araujo et al. (2022) considered the performance analysis of water and 1-ethyl-3-methylimidazolium-based ionic liquid mixtures in an absorption refrigeration system. The work provides an alternative to the conventional water/LiBr absorption refrigeration system that has crystallization issues.

Gao et al. (2021) considered sorption cold energy storage and transmission using ionic liquid absorbents. Li et al. (2021) studied the viscosity characteristics of carbon-di-oxide-ionic liquid mixtures that could be applied in absorption refrigeration systems. In this work, the effects of carbon-di-oxide solubility, pressure, temperature, and ionic-liquid molecular arrangement on the blend viscosity were examined. Zhai et al. (2021) considered the performance and optimization of absorption heat pumps using ionic liquids. The performance of five different ionic liquid-water mixtures was considered in this work. Ayad et al. (2021) determined the thermodynamic properties of tricyanomethanide-based ionic liquids that could potentially be used for absorption heat transformers. Bergman et al. listed several relationships required for modeling the thermal performance of heat exchanger systems. A few relationships listed therein were used in this work. Likewise, McQuiston et al. (2004) presented analysis and standards to be used in air conditioning systems and these have been applied in this work.

## 2  Project Description

In the design of the air conditioning process, the room (lab) total heat must be determined. Room total heat consists of heat transmitted from walls, windows and heat generated in the room itself. This heat must be removed to maintain a steady comfortable condition in the room.

### 2.1 Room Total Heat

Due to solar radiation, it is assumed that the average temperature that the walls and windows are exposed to is 55°C which is representative of Al Ahsa, Saudi Arabia. Radiation is treated as a surface phenomenon and solar radiation heats up the surface of walls and windows on the exterior side.

The temperature difference between the surfaces of the wall/windows serves as the driving potential for heat transfer. It is also assumed that the wall is made out of bricks and the windows consist of double glass panes separated by means of an air gap.
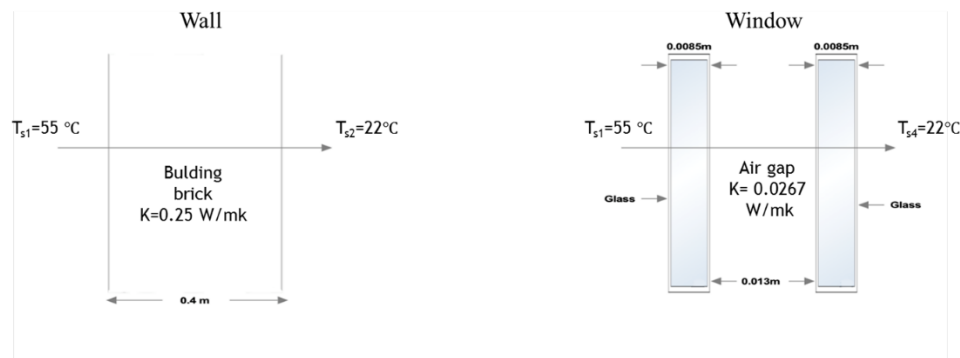


**Figure 1**: Wall and window dimensions

Per Bergman et al. the rate of heat transfer through the wall can be given as

$$q_{wall} = \frac{\Delta T}{\left[\frac{L}{kA}\right]_{wall}},$$   (1),

where

L – thickness (m)

k – thermal conductivity (W/mK)

A – area normal to heat flow (m$^2$)

The rate of heat transfer through the walls was determined to be 587 W. The rate of heat transfer through the windows can be given per Bergman et al. as

$$q_{windows} = \frac{\Delta T}{\left[\frac{L}{kA}\right]_{glass} + \left[\frac{L}{kA}\right]_{airgap} + \left[\frac{L}{kA}\right]_{glass}} * \# \text{ of windows},$$   (2).

The rate of heat transfer through the windows was determined to be 223 W. The heat transfer through walls and windows can be classified as sensible heat.

Heat is also generated within the room through electrical instruments and humans. Humans add both sensible and latent heat to the room. The total amount of heat generated in the room from humans can be determined as

$$q_{people} = [\text{sensible heat} + \text{latent heat}] * \# \text{ of people},$$   (3)

As per ASHRAE STD 55 (2017) from McQuiston et al. (2004) for humans within the work environment where no physical activity is involved, the average amount of sensible heat and latent heat generated by a person is ~90 W and 60 W, respectively. The maximum number of people in the lab was arbitrarily considered as 30. Thus, the total heat generated in the room from humans is ~4500 W. In addition, there are 64 electric bulbs having a rating of 85 W. Therefore, the sensible heat generated in the room from electric bulbs is 5440 W. The net heat load in the room is presented in Table 1.

**Table 1:** Heat load in the room

| Item | Sensible heat (W) | Latent Heat (W) |
|------|------------------|-----------------|
| People | 2700 | 1800 |
| Light | 5440 | 0 |
| Glass | 223 | 0 |
| Wall | 587 | 0 |
| **Total** | **8950** | **1800** |

It can be seen that the total heat generated in the lab is 10.75 kW.

## 2.2 Project Constraints

The constraints for the air conditioning project are described in Table 2.

**Table 2:** Project Constraints

| S. No | Item | Description |
|-------|------|-------------|
| 1 | Apply ASHRAE STD 55 (2017), human comfort temp condition, per McQuiston et al. | 22°C -26°C |
| 2 | Apply ASHRAE STD55 (2017), human comfort relative humidity (RH), per McQuiston et al. | 50% - 55% |
| 3 | Outside air for freshness per ASHRAE 62.1 – 2013, per McQuiston et al. | 0.142 (m3/min)/person |
| 4 | Remove the generated heat in the room | 10.75 kW (at least) |

# 3 Design of Air Conditioning Process

Herein, based on industry practice, a psychrometric chart was used to design the air conditioning process. The psychrometric chart is described in Figure 2. The various properties pertaining to comfort air conditioning are depicted in the chart. As an example, properties are presented for air at 40°C and 20% RH.
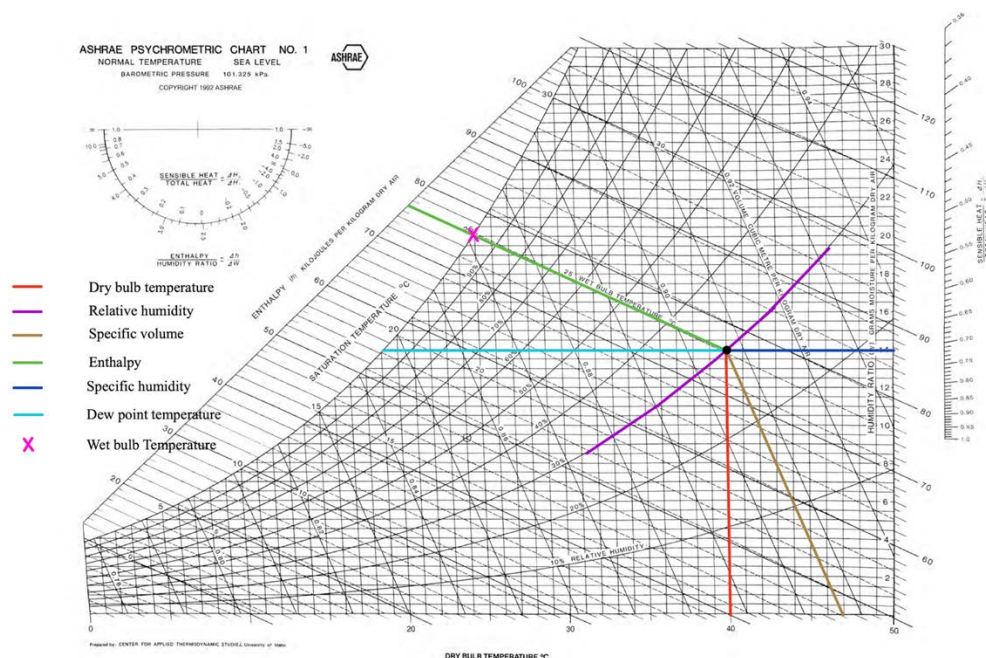


**Figure 2**: Psychrometric chart (McQuiston et al., 2004)

As per the requirement, a certain amount of fresh air is inducted into the air conditioning system. The fresh air requirement is described in Table 2. The mixing of fresh air with room air can occur either before or after the cooling coil.
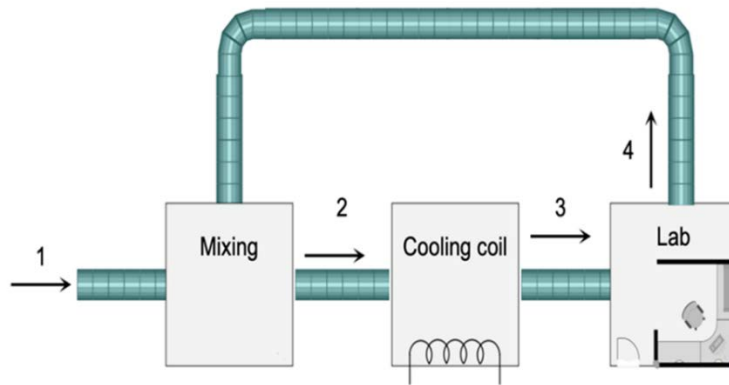
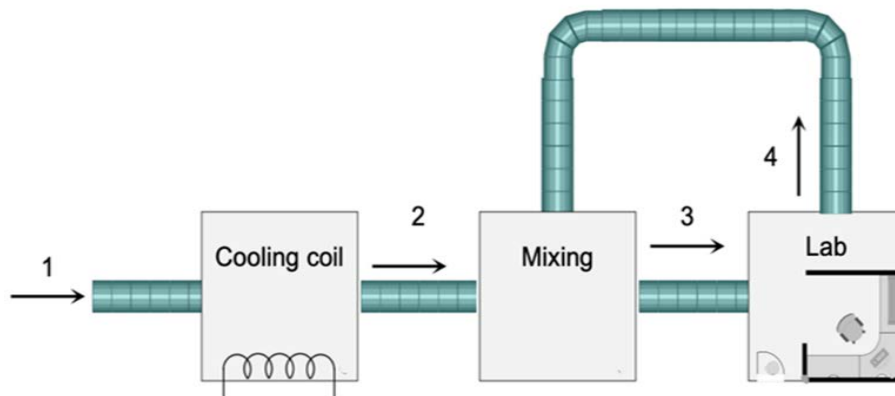**Figure 3:** Mixing of fresh air with re-circulated air before the cooling coil - considered for summer air conditioning (air conditioning process layout)



**Figure 4:** Mixing of fresh air with re-circulated air after the cooling coil (air conditioning process layout)

In this work, a comparative study between chilled water and ionic liquid-water mixtures was examined as the coolant. The design alternatives and mixing proportions examined are given in Tables 3 and 4.

**Table 3:** Design Alternatives

| S. No | Item | Options |
|-------|------|---------|
| 1 | Air conditioning design | Psychrometric relations (or) psychrometric chart |
| 2 | Mixing | Fresh air mixing before cooling coil (or) Fresh air mixing after cooling coil |
| 3 | Coolant for the cooling coil | Chilled H2O (or) ionic liquid-water mixtures |

Various mixing proportions (by mass) are considered and they are described in Table 4.

**Table 4:** Mixing proportions considered

| Case | Fresh Air | Recirculated Air |
|------|-----------|------------------|
| 1 | 0% | 100% (base line) |
| 2 | 5% | 95% |
| 3 | 10% | 90% |

For brevity, the detailed procedure in designing the air conditioning process is described only for case 2, where the mixing of 5% fresh air with 95% recirculated air was studied. Per McQuiston et al. (2004) RSHF is defined as

$$RSHF = \frac{\text{Room sensible heat (RSH)}}{\text{Room total heat (RTH)}}, .. \qquad (4).$$
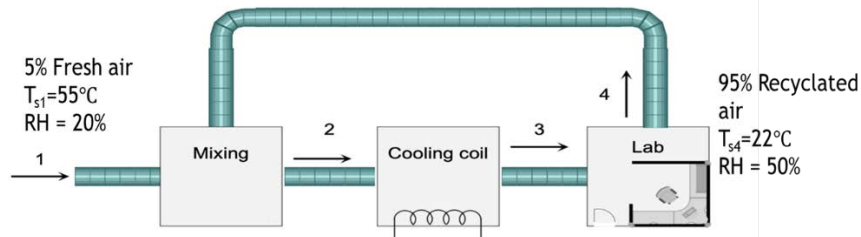


**Figure 5:** Air conditioning process layout – case 2

Per McQuiston et al. the room total heat (RTH) is the summation of room sensible heat (RSH) and room latent heat (RLH).

$$RTH = RSH + RLH, \qquad (5)$$

The determination of RSHF is described in Table 5.

**Table 5:** Determination of RSHF

| S. No | Item | Description |
|-------|------|-------------|
| 1 | RTH | 10.75 KW |
| 2 | RSH | 8.95 KW |
| 3 | RLH | 1.8 KW |
| 4 | RSHF | 0.833 |

RSHF is then plotted in the sensible heat factor (SHF) scale in the Psychrometric chart.
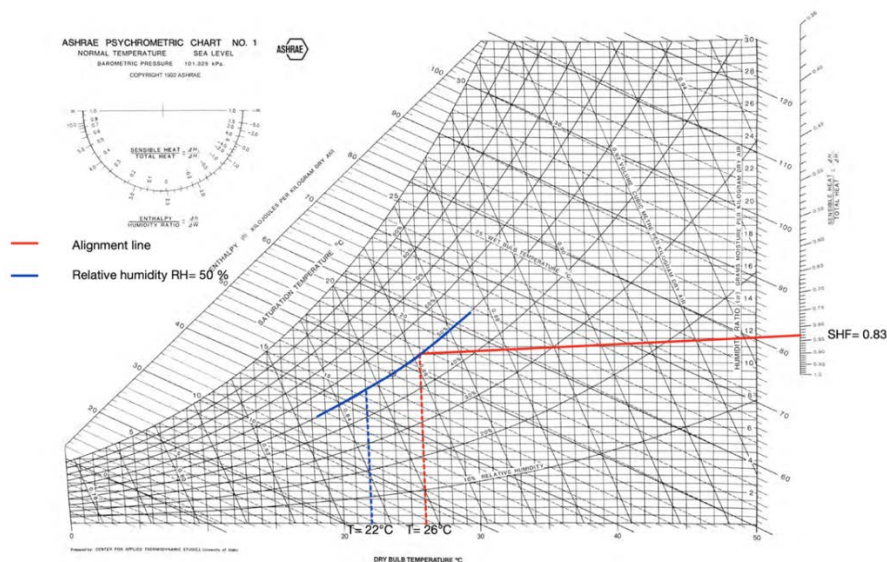


**Figure 6:** Air conditioning process – case 2; psychrometric chart (McQuiston et al., 2004).

RSHF is connected with the ASHRAE human comfort point, 26°C and 50% RH described in the psychrometric chart. This line is termed the alignment line. RSHF line is then constructed by drawing a line parallel to the alignment line and through the room (lab) condition. Room comfort condition is chosen as 22°C and 50% RH. All possible room supply conditions lie in the RSHF line.

Considering Figure 5, it is required to determine the mixed condition 2. The mixing of fresh air with recirculated air is described in Figure 7.
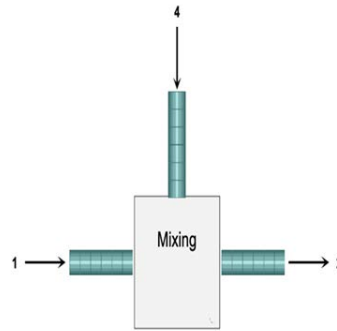


**Figure 7:** Mixing of fresh air 1 with recirculation air 4

Mixed condition 2, can be determined by applying the concepts such as mass balance, energy balance and water balance.

Considering the mixing chamber as a control volume, per McQuiston et al. the mass balance is given as

$$\dot{m}_1 + \dot{m}_4 = \dot{m}_2 \tag{6}.$$

Applying energy balance to mixing yields

$$\dot{m}_1 h_1 + \dot{m}_4 h_4 = \dot{m}_2 h_2 \tag{7}.$$

Likewise, applying water balance to mixing yields

$$\dot{m}_1 \omega_1 + \dot{m}_4 \omega_4 = \dot{m}_2 \omega_2 \tag{8},$$

where

$\dot{m}$ – mass flow rate of air (kg/s)

h – enthalpy of moist air (kJ/kg)

$\omega$ – specific humidity (kg of water/kg of air)

Applying the above equations, the mixed condition is determined and is presented in Table 6.

**Table 6:** Mixed condition – case 2; 95% recirculated air & 5% fresh air

| S. No | Item | Description |
|-------|------|-------------|
| 1 | $\omega 2$ | 0.00878 kg. of H2O/kg. of air |
| 2 | T2 | 23°C |
| 3 | h2 | 46.2 kJ/kg |
| 4 | RH2 | 50% |

The supply air to the room (lab) must be able to displace the heat infiltrated & heat generated in the room and must maintain stipulated human comfort conditions. The Grand sensible heat factor (GSHF) line describes the condition of air as it moves through the cooling coil. Per McQuiston et al. (2004), GSHF line in the psychrometric chart connects the cooling coil inlet

condition (mixed condition 2), cooling coil surface temperature and cooling coil's discharge condition (room supply condition 3).

The surface temperature of the cooling coil is termed apparatus dew point temperature (ADP). ADP lies on the saturation curve and is below the DPT of room comfort condition. The cooling coil surface temperature is assumed as 9°C. Herein, the mixed condition, point 2 and ADP are known. Therefore, GSHF line can be constructed using the two known conditions. GSHF line will intersect RSHF line. The intersection of RSHF line and GSHF line provides the best supply condition. The process is described in Figure 8.

The procedure was repeated for all the cases and the results are provided in Tables 7 & 8. Case 3 (highlighted in green) is chosen for the air conditioning process as it satisfies the fresh air criterion.
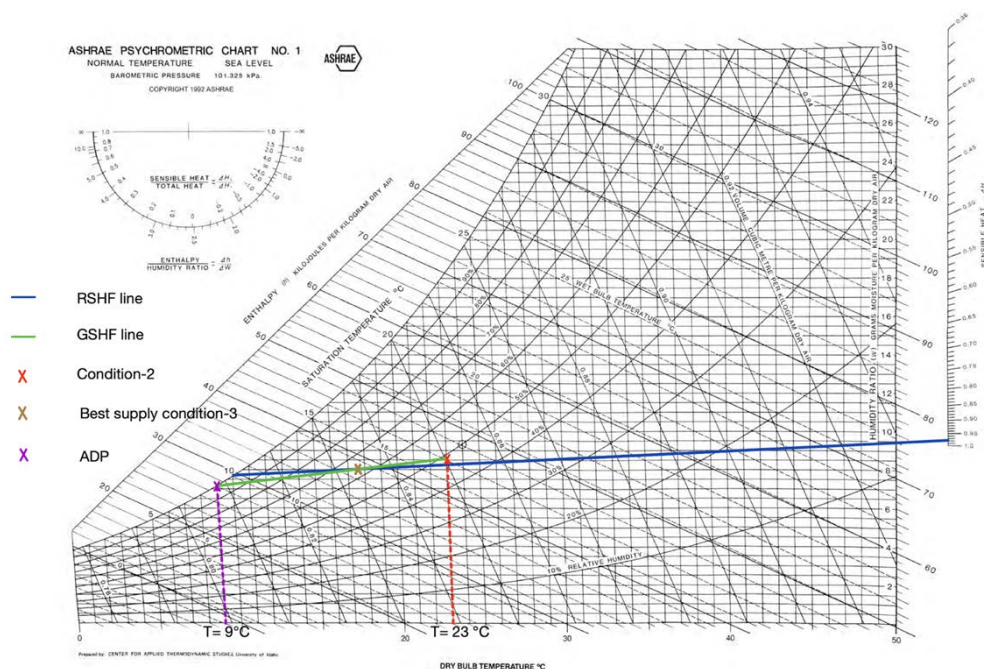


**Figure 8:** Estimation of best supply condition; psychrometric chart (McQuiston et al., 2004)

**Table 7:** Results – design of air conditioning process

| Case # | Mixing | | Room Supply Condition | | Mass Flow Rate | | |
|--------|--------|--------|--------|--------|--------|--------|--------|
| | Fresh Air (%) | Room Air (%) | Temp (°C) | RH (%) | Fresh Air (kg/s) | Recirculated Air (kg/s) | Supply Air (kg/s) |
| 1 | 0 | 100 | 14 | 78 | 0 | 1.13 | 1.13 |
| 2 | 5 | 95 | 14 | 78 | 0.0565 (0.1 m3/min/person) | 1.074 | 1.13 |
| 3 | 10 | 90 | 13 | 82 | 0.1 (0.178 m3/min/person) | 0.9 | 1 |

From Table 2, it can be seen that the requirement for fresh air must be at least 0.142 (m³/min)/person. This constraint is satisfied in case 3 when 10% of fresh air is inducted into the air conditioning system. Table 8 describes the load on the cooling coil.

**Table 8:** Results – load on the cooling coil

| Case # | Mixing Fresh Air (%) | Room Air (%) | Heat carried by fresh air (KW) | Heat carried by recirculated air (KW) | Total heat (KW) | Load on cooling coil (KW) | Error |
|---|---|---|---|---|---|---|---|
| 1 | 0 | 100 | 0 | 10.75 | 10.75 | 10.75 | 0% |
| 2 | 5 | 95 | 3.62 | 10.20 | 13.82 | 14.35 | 3.8% |
| 3 | 10 | 90 | 6.4 | 9.72 | 16.12 | 16.2 | 0.5% |

The error in estimating the load on the cooling coil is due to the usage of the psychrometric chart in the air conditioning design process. The summary of the air conditioning design for the lab is detailed in Table 9.

**Table 9:** Summary of air conditioning design for the lab

| S. No | Item | Description |
|---|---|---|
| 1 | Room (lab) Temperature | 22°C |
| 2 | Relative humidity (RH) | 50% |
| 3 | Max. number of people in the lab | 30 |
| 4 | Outside air for freshness | 0.178 (m3/min)/person |
| 5 | Design methodology | Psychrometric chart |
| 6 | Mixing chamber | Located before cooling coil |
| 7 | Mixing proportion | 10% fresh air 90% recirculated air |
| 8 | Supply condition of air | 13°C, 82% RH, & 0.1 kg/s |
| 9 | The total load on cooling coil | 16.2 kW |

# 4  Design of Cooling Coil

The design of the cooling coil using chilled water and ionic liquid-water mixtures is examined in this section. A typical cross-flow heat exchanger is described in Figure 9.
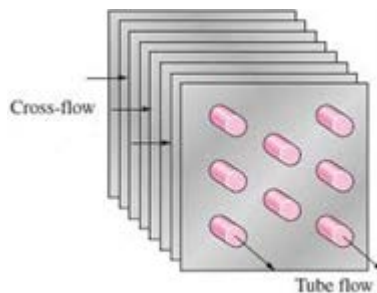


**Figure 9:** Cross flow heat exchanger, from Bergman et al.

In this analysis, the air is the external fluid that flows over the tubes, and the secondary refrigerant (or) the coolant flows through the tubes. In each instance, the cooling performance of the ionic liquid-water mixture was compared with that of chilled water. The required mass flow rate of air, the mass flow rate of coolant, the required inlet and discharge temperatures for air and coolant, and the thermal properties of fluids are all known quantities. Thermal properties of fluids were assumed constant. External fluid flow was considered unmixed, and the tube side fluid flow was considered mixed. Likewise, the overall number of transfer units (NTU) was anticipated to be equally spread among the heat exchanger passes. In this project work, a 3-pass cross-flow heat

exchanger is considered. In a 3-pass cross flow heat exchanger, each tube side fluid element streams through the entire length of the heat exchanger 3 times before exiting the heat exchanger.
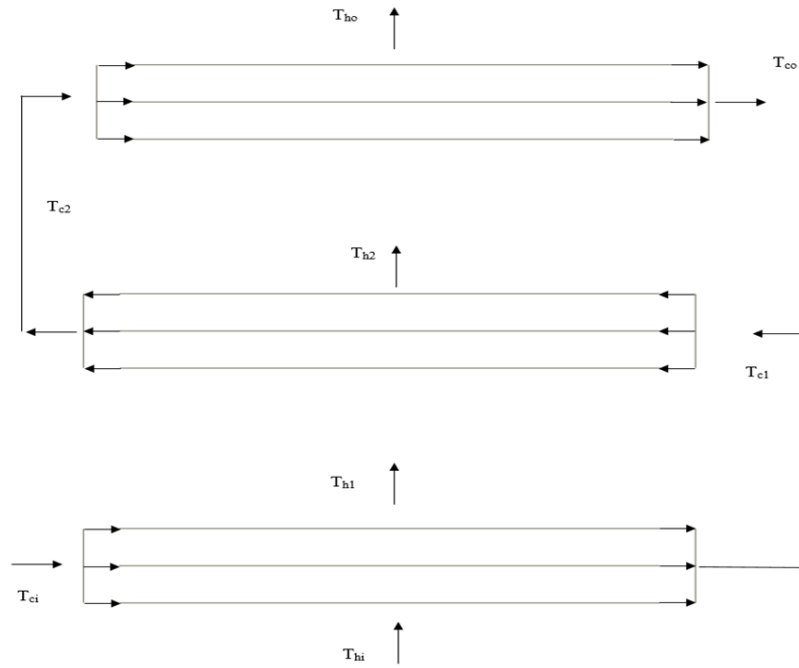


**Figure 10:** 3-pass cross flow heat exchanger

Per Bergman et al. the capacity rate of air (external fluid, hot) is given as

$$C_h = C_{air} = \dot{m}_{air} c_{p,air}, \tag{9}.$$

Likewise, the capacity rate of coolant (tube side fluid, cold) is given as

$$C_c = C_{coolant} = \dot{m}_{coolant} c_{p,coolant}, \tag{10}.$$

If $C_{air} > C_{coolant}$, then, $C_{air}$ will be the maximum capacity rate fluid and shall be denoted as $C_{max}$. In this case, $C_{coolant}$ will be the minimum capacity rate fluid and shall be identified as $C_{min}$. Likewise, if $C_{air} < C_{coolant}$, then, $C_{air}$ will be the minimum capacity rate fluid and shall be given as $C_{min}$. In this case, $C_{coolant}$ will be the maximum capacity rate fluid and shall be designated as $C_{max}$. The capacity rate ratio ($C_r$) is a dimensionless parameter that connects the capacity rate of both fluids employed in the heat exchanger. Since the specific heats and flow rates of both fluids are known, the overall capacity rate ratio can be readily determined. Per Bergman et al. the overall capacity rate ratio may be given as

$$C_r = \frac{C_{min}}{C_{max}} \tag{11}.$$

The capacity rate ratio per heat exchanger pass would be the same as the overall capacity rate ratio, as each heat exchanger pass is subjected to the full mass flow rate of air and secondary refrigerant (coolant).

$$C_r = C_r' \tag{12},$$

where $C_r'$ – capacity rate ratio per pass.

The number of transfer units (NTU) is a dimensionless parameter that accounts for heat exchanger surface area, flow rates, material properties, fluid properties, fouling, etc. The typical NTU of heat exchangers used in steady state sensible heat transfer applications is typically less than 4. The number of transfer units (NTU) is given through the following relationship.

$$NTU = \frac{U_o A_o}{C_{min}} \tag{13},$$

where

NTU – number of transfer units

$A_o$ – overall outside surface area

Uo – overall heat transfer coefficient (W/m$^2$K)

In this project, the overall NTU is assumed as a known quantity and is varied until the desired output is attained. The NTU per pass may be assumed as

$$NTU' = \frac{NTU}{n} \tag{14},$$

where

NTU' – NTU per pass

n – number of passes (for this project n = 3)

For a cross-flow heat exchanger, per Bergman et al. an analytical relationship correlates heat exchanger effectiveness, NTU, and $C_r$. The overall heat exchanger effectiveness is given as

$$\varepsilon = \left(\frac{1}{Cr}\right)(1 - \exp(-Cr[1 - \exp(-NTU)]\}) \tag{15}.$$

Similarly, the effectiveness of each heat exchanger pass may be linked to the capacity rate ratio per pass and NTU per pass and is given as

$$\varepsilon' = \left(\frac{1}{C_r'}\right)(1 - \exp(-C_r'[1 - \exp(-NTU')]\}), \tag{16},$$

where ε' – effectiveness per pass

## 4.1 Estimation of Exit Temperatures of Fluids from the Cross Flow Heat Exchanger

The properties of air, water, ionic liquid-water mixtures, and inlet conditions to the cross-flow heat exchanger are presented in Table 10.

Consider Figure 10 describing a 3-pass cross-flow heat exchanger. In the subsequent equations, subscript "h" refers to the hot fluid, air, and subscript "c" refers to the cold fluid, water. Subscript "1" and "2" refers to the exit condition at the 1st and 2nd pass respectively. Likewise, the subscript "i" and "o" refers to the condition at the inlet and exit of the cross-flow heat exchanger. Applying energy balance to first pass yields

$$(\dot{m}c_p)_h * (T_{hi} - T_{h1}) = (\dot{m}c_p)_c * (T_{c1} - T_{ci}) \tag{17}.$$

**Table 10:** Properties of fluids and inlet conditions to cross flow heat exchanger

| Item | External fluid Hot fluid | Internal (tube side) fluid - Coolant | | | | |
|------|------|------|------|------|------|------|
| | Air | Water | $[P_{14,6,6,6}]$ [ButO] + 16.680% water (w/w) | $[P_{14,6,6,6}]$ [HexO] + 15.825% water (w/w) | $[P_{14,6,6,6}]$ [OctO] + 14.783% water (w/w) | $[P_{14,6,6,6}]$ [DecO] + 14.150% water (w/w) |
| Specific heat $c_p$ (J/kg.K) | 1005.0 | 4190.0 | 3400.0 | 3300.0 | 3100.0 | 2900.0 |
| Density $\rho$ (kg/m$^3$) | 1.2 | 1000.0 | 910.0 | 908.0 | 902.0 | 900.0 |
| Dynamic viscosity $\mu$ (Pa-s) | 1.8E-05 | 1.4E-03 | 6.0E-02 | 8.0E-02 | 8.2E-02 | 9.2E-02 |
| Prandtl number Pr | 0.7 | 10.6 | 1073.7 | 1411.8 | 1359.4 | 1434.4 |
| Kinematic viscosity $\nu$ (m$^2$/s) | 1.5E-05 | 1.4E-06 | 6.6E-05 | 8.8E-05 | 9.1E-05 | 1.0E-04 |
| Thermal conductivity K (W/m.K) | 0.026 | 0.575 | 0.190 | 0.187 | 0.187 | 0.186 |
| Mass flow rate (kg/hr) | 3600.0 | 6908.4 | 6908.4 | 6908.4 | 6908.4 | 6908.4 |
| Inlet temp $T_{in}$ (°C) | 25.0 | 8.0 | 8.0 | 8.0 | 8.0 | 8.0 |

Upon rearranging, yields

$$T_{c1} + C_r * T_{h1} = T_{ci} + C_r * T_{hi} \tag{18}$$

Applying energy balance to the second pass yields

$$(\dot{m}c_p)_h * (T_{h1} - T_{h2}) = (\dot{m}c_p)_c * (T_{c2} - T_{c1}) \tag{19}$$

Upon rearranging yields

$$T_{c2} + C_r * T_{h2} - T_{c1} - C_r * T_{h1} = 0 \tag{20}$$

Applying energy balance to the third pass yields

$$(\dot{m}c_p)_h * (T_{h2} - T_{ho}) = (\dot{m}c_p)_c * (T_{co} - T_{c2}) \tag{21}$$

Upon rearranging yields

$$T_{co} + C_r * T_{ho} - T_{c2} - C_r * T_{h2} = 0 \tag{22}$$

Applying effectiveness to first pass yields

$$\mathcal{E}' = \frac{q}{q_{max}} = \frac{q}{C_{min} * [\Delta T]_i} = \frac{C_{min} * [T_{hi} - T_{h1}]}{C_{min} * [T_{hi} - T_{ci}]} = \frac{[T_{hi} - T_{h1}]}{[T_{hi} - T_{ci}]} \tag{23}$$

Upon rearranging yields

$$T_{h1} = T_{hi} - \mathcal{E}' * [T_{hi} - T_{ci}] \tag{24}$$

Applying effectiveness to second pass yields

$$\mathcal{E}' = \frac{q}{q_{max}} = \frac{q}{C_{min} * [\Delta T]_i} = \frac{C_{min} * [T_{h1} - T_{h2}]}{C_{min} * [T_{h1} - T_{c1}]} = \frac{[T_{h1} - T_{h2}]}{[T_{h1} - T_{c1}]} \tag{25}$$

Upon rearranging yields

$$T_{h2} - T_{h1} + \mathcal{E}' * [T_{h1} - T_{c1}] = 0 \tag{26}$$

Applying effectiveness to third pass yields

$$\varepsilon' = \frac{q}{q_{max}} = \frac{q}{C_{min}*[\Delta T]_i} = \frac{C_{min}*[T_{h1}-T_{ho}]}{C_{min}*[T_{h2}-T_{c2}]} = \frac{[T_{h2}-T_{ho}]}{[T_{h2}-T_{c2}]} \qquad (27).$$

Upon rearranging yields

$$T_{ho} - T_{h2} + \varepsilon' * [T_{h2} - T_{c2}] = 0 \qquad (28).$$

The four intermediary temperatures and two discharge temperatures can be determined by solving Equations 18, 20, 22, 24, 26, and 28. The six simultaneous linear equations may be given in matrix form as

$$\begin{bmatrix} C_r & 0 & 0 & 1 & 0 & 0 \\ C_r & -C_r & 0 & 1 & -1 & 0 \\ 0 & C_r & -C_r & 0 & 1 & -1 \\ 1 & 0 & 0 & 0 & 0 & 0 \\ \varepsilon'-1 & 1 & 0 & -\varepsilon' & 0 & 0 \\ 0 & \varepsilon'-1 & 1 & 0 & -\varepsilon' & 0 \end{bmatrix} \begin{bmatrix} T_{h1} \\ T_{h2} \\ T_{ho} \\ T_{c1} \\ T_{c2} \\ T_{co} \end{bmatrix} = \begin{bmatrix} T_{ci} + C_r * T_{hi} \\ 0 \\ 0 \\ T_{hi} - \varepsilon' * [T_{hi} - T_{ci}] \\ 0 \\ 0 \end{bmatrix} \qquad (29).$$

The simultaneous linear equations can be readily modeled in MATLAB to yield intermediary and discharge temperatures.

A parametric study was conducted by varying the NTU to obtain the desired heat exchanger output, (i.e.) 13°C on the air (external) side of the heat exchanger. Since the cooling coil is maintained at ADP, if the heat exchanger is designed to remove sensible heat, the necessary removal of latent heat is automatically taken care of through condensation. The results from the parametric study are described in the tables below. The required NTU to achieve the desired output temperature is highlighted in blue.

**Table 11:** Performance of 3-pass cross flow heat exchanger – air and chilled water

| S.No | NTU | Cr | Tair, in (K) | Twater, in (K) | Tair, out (°C) | Twater, out (°C) |
|------|-----|------|------|------|------|------|
| 1 | 0.1 | 0.125 | 298 | 281 | 23.4 | 8.2 |
| 2 | 0.2 | 0.125 | 298 | 281 | 22.0 | 8.4 |
| 3 | 0.4 | 0.125 | 298 | 281 | 19.5 | 8.7 |
| 4 | 0.6 | 0.125 | 298 | 281 | 17.6 | 8.9 |
| 5 | 0.8 | 0.125 | 298 | 281 | 16.0 | 9.1 |
| 6 | 1 | 0.125 | 298 | 281 | 14.6 | 9.3 |
| 7 | 1.1 | 0.125 | 298 | 281 | 14.1 | 9.4 |
| 8 | 1.2 | 0.125 | 298 | 281 | 13.6 | 9.4 |
| 9 | 1.3 | 0.125 | 298 | 281 | 13.1 | 9.5 |
| 10 | 1.4 | 0.125 | 298 | 281 | 12.7 | 9.5 |

**Table 12:** Performance of 3-pass cross flow heat exchanger – air and [P$_{14,6,6,6}$] [ButO] + 16.680% water (w/w)

| S.No | NTU | Cr | T$_{air, in}$ (K) | T$_{ButO, in}$ (K) | T$_{air, out}$ (°C) | T$_{ButO, out}$ (°C) |
|------|-----|------|------|------|------|------|
| 1 | 0.1 | 0.154 | 298 | 281 | 23.4 | 8.2 |
| 2 | 0.2 | 0.154 | 298 | 281 | 22.0 | 8.5 |
| 3 | 0.4 | 0.154 | 298 | 281 | 19.6 | 8.8 |
| 4 | 0.6 | 0.154 | 298 | 281 | 17.6 | 9.1 |
| 5 | 0.8 | 0.154 | 298 | 281 | 16.0 | 9.4 |
| 6 | 1 | 0.154 | 298 | 281 | 14.7 | 9.6 |
| 7 | 1.1 | 0.154 | 298 | 281 | 14.2 | 9.7 |
| 8 | 1.2 | 0.154 | 298 | 281 | 13.7 | 9.7 |
| 9 | 1.3 | 0.154 | 298 | 281 | 13.2 | 9.8 |
| 10 | 1.4 | 0.154 | 298 | 281 | 12.8 | 9.9 |

**Table 13:** Performance of 3-pass cross flow heat exchanger: air and [P$_{14,6,6,6}$] [HexO] + 16.680% water (w/w)

| S.No | NTU | Cr | Tair, in (K) | THexO, in (K) | Tair, out (℃) | THexO, out (℃) |
|------|-----|-----|------|------|------|------|
| 1 | 0.1 | 0.159 | 298 | 281 | 23.4 | 8.2 |
| 2 | 0.2 | 0.159 | 298 | 281 | 22.0 | 8.5 |
| 3 | 0.4 | 0.159 | 298 | 281 | 19.6 | 8.8 |
| 4 | 0.6 | 0.159 | 298 | 281 | 17.6 | 9.1 |
| 5 | 0.8 | 0.159 | 298 | 281 | 16.0 | 9.4 |
| 6 | 1 | 0.159 | 298 | 281 | 14.7 | 9.6 |
| 7 | 1.1 | 0.159 | 298 | 281 | 14.2 | 9.7 |
| 8 | 1.2 | 0.159 | 298 | 281 | 13.7 | 9.7 |
| 9 | 1.3 | 0.159 | 298 | 281 | 13.2 | 9.8 |
| 10 | 1.4 | 0.159 | 298 | 281 | 12.8 | 9.9 |

**Table 14:** Performance of 3-pass cross flow heat exchanger – air and [P$_{14,6,6,6}$] [OctO] + 16.680% water (w/w)

| S.No | NTU | Cr | Tair, in (K) | TOctO, in (K) | Tair, out (℃) | TOctO, out (℃) |
|------|-----|-----|------|------|------|------|
| 1 | 0.1 | 0.169 | 298 | 281 | 23.4 | 8.2 |
| 2 | 0.2 | 0.169 | 298 | 281 | 22.0 | 8.5 |
| 3 | 0.4 | 0.169 | 298 | 281 | 19.6 | 8.8 |
| 4 | 0.6 | 0.169 | 298 | 281 | 17.6 | 9.1 |
| 5 | 0.8 | 0.169 | 298 | 281 | 16.1 | 9.4 |
| 6 | 1 | 0.169 | 298 | 281 | 14.8 | 9.6 |
| 7 | 1.1 | 0.169 | 298 | 281 | 14.2 | 9.7 |
| 8 | 1.2 | 0.169 | 298 | 281 | 13.7 | 9.7 |
| 9 | 1.3 | 0.169 | 298 | 281 | 13.3 | 9.8 |
| 10 | 1.4 | 0.169 | 298 | 281 | 12.8 | 9.9 |

**Table 15:** Performance of 3-pass cross flow heat exchanger – air and [P$_{14,6,6,6}$] [DecO] + 16.680% water (w/w)

| S.No | NTU | Cr | Tair, in (K) | TDecO, in (K) | Tair, out (℃) | TDecO, out (℃) |
|------|-----|-----|------|------|------|------|
| 1 | 0.1 | 0.181 | 298 | 281 | 23.4 | 8.2 |
| 2 | 0.2 | 0.181 | 298 | 281 | 22.0 | 8.5 |
| 3 | 0.4 | 0.181 | 298 | 281 | 19.6 | 8.8 |
| 4 | 0.6 | 0.181 | 298 | 281 | 17.7 | 9.1 |
| 5 | 0.8 | 0.181 | 298 | 281 | 16.1 | 9.4 |
| 6 | 1 | 0.181 | 298 | 281 | 14.8 | 9.6 |
| 7 | 1.1 | 0.181 | 298 | 281 | 14.3 | 9.7 |
| 8 | 1.2 | 0.181 | 298 | 281 | 13.8 | 9.7 |
| 9 | 1.3 | 0.181 | 298 | 281 | 13.3 | 9.8 |
| 10 | 1.4 | 0.181 | 298 | 281 | 12.9 | 9.9 |

**Table 16:** Performance summary of 3-pass cross flow heat exchanger – air and various coolants

| Item | Cr | NTU | Inlet Temperatures | | Outlet Temperatures | |
|------|-----|-----|------|------|------|------|
| | | | Thi (℃) | Tci (℃) | Tho (℃) | Tco (℃) |
| Air + chilled water | 0.125 | 1.3 | 25.0 | 8.0 | 13.09 | 9.49 |
| Air + [P14,6,6,6] [ButO] + 16.680% water (w/w) | 0.154 | 1.4 | 25.0 | 8.0 | 12.78 | 9.88 |
| Air + [P14,6,6,6] [HexO] +15.825% water (w/w) | 0.159 | 1.4 | 25.0 | 8.0 | 12.80 | 9.88 |
| Air + [P14,6,6,6] [OctO] + 14.783% water (w/w) | 0.169 | 1.4 | 25.0 | 8.0 | 12.84 | 9.87 |
| Air + [P14,6,6,6] [DecO] +14.150% water (w/w) | 0.181 | 1.4 | 25.0 | 8.0 | 12.88 | 9.87 |

A comparison between chilled water and selected ionic liquid-water mixtures for the given air conditioning application indicates that both chilled water and ionic liquid-water mixtures require nearly the same NTU to provide the necessary cooling. It is a common practice in heat exchanger industries to fix the required capacity rate ratio, NTU, and the heat exchanger effectiveness before deducing the detailed design of the heat exchanger. Since the NTU requirement is about the same, the design of the cross-flow heat exchanger would be similar concerning the usage of chilled water or ionic liquid-water mixtures.

# 5 Conclusion

This paper addresses the design of an air conditioning system. ASHRAE standards describing human comfort conditions were considered in the study. For convenience, a Psychrometric chart was used for the design analysis. Different alternatives were presented and an optimal design consisting of a suitable layout, fresh air intake, and best supply condition was determined. Though air conditioning design seems like a straightforward engineering study, a lot of considerations must be taken into account while designing an air conditioning system. The paper tries to highlight the main points that must be taken into account while designing an air conditioning system. A detailed stepwise procedure for designing the air conditioning process is yet to be documented in the technical literature.

The air conditioning design projected the load on the cooling coil. Since the project deals with gas-to-liquid heat transfer applications, a finned cross-flow heat exchanger is considered. Chilled water and various ionic liquid-water mixtures were considered suitable coolants. Chilled water has been used for decades as a secondary refrigerant for air conditioning purposes. Chilled water is safe, easy to pump, has a higher heat-bearing capability, and its leakages can be tolerated. The use of ionic liquid-water mixtures for sensible heating and cooling applications is still in the research stage and hasn't yet been commercially implemented in practical applications. The current chemical cost is quite high, for example, 50g of ionic liquid may cost around £110. But once the ionic liquids are commercialized, the costs are expected to come down. Nevertheless, the initial setup cost for erecting cooling systems using ionic liquid-water mixtures is expected to be significantly higher than those systems employing water.

One of the advantages of using ionic liquid-water mixtures is that the properties of the ionic liquid-water mixtures can be easily improved by adjusting the concentration of water as well as by changing the chemical structure of anion and cation. Nevertheless, the results presented are based on the properties available in the literature. For the selected application, and under the given conditions, chilled water and ionic liquid-water mixtures deliver similar performance. Recognize that ionic liquid-water mixtures have desirable properties such as lower freezing temperature, lower vapor pressure, energy storage, etc. The results from this work are encouraging, and in the future, the ionic liquid-water mixtures may have the potential to replace water in certain cooling and heating applications. The results presented in this work are purely from an analytical approach, using well-established fundamental and empirical equations.

# 6  Availability of Data and Material

Data can be made available by contacting the corresponding author.

# 7  Acknowledgement

# 8  References

Oster K, Goodrich P, Jacquemin J, Hardacre C, Ribeiro AP, Elsinawi A. A new insight into pure and water-saturated quaternary phosphonium-based carboxylate ionic liquids: Density, heat capacity, ionic conductivity, thermogravimetric analysis, thermal conductivity and viscosity. The Journal of Chemical Thermodynamics. 2018 Jun 1;121:97-111.

Oster K, Jacquemin J, Hardacre C, Ribeiro AP, Elsinawi A. Further development of the predictive models for physical properties of pure ionic liquids: Thermal conductivity and heat capacity. The Journal of Chemical Thermodynamics. 2018 Mar 1;118:1-5.

Cherecheş EI, Minea AA. Experimental evaluation of electrical conductivity of ionanofluids based on water–[C2mim][CH3SO3] ionic liquids mixtures and alumina nanoparticles. Journal of Thermal Analysis and Calorimetry. 2021 Sep;145(6):3151-7.

Nimmagadda R, Chereches EI, Chereches M. Heat Transfer Performance of Uni-Directional and Bi-Directional Lid-Driven Cavities Using Nanoparticle Enhanced Ionic Liquids (NEILS). International Journal of Thermophysics. 2021 May;42(5):1-8.

Haddad AZ, Menon AK, Kang H, Urban JJ, Prasher RS, Kostecki R. Solar Desalination using thermally responsive ionic liquids regenerated with a photonic heater. Environmental science & technology. 2021 Feb 17;55(5):3260-9.

El-Sinawi A, Silaipillayarputhur K, Al-Mughanam T, Hardacre C. Performance of ionic liquid-water mixtures in an acetone cooling application. Sustainability. 2021 Mar 9;13(5):2949.

Cherecheş EI, Prado JI, Cherecheş M, Minea AA, Lugo L. Experimental study on thermophysical properties of alumina nanoparticle enhanced ionic liquids. Journal of Molecular Liquids. 2019 Oct 1;291:111332.

Asensio-Delgado S, Pardo F, Zarca G, Urtiaga A. Absorption separation of fluorinated refrigerant gases with ionic liquids: Equilibrium, mass transport, and process design. Separation and Purification Technology. 2021 Dec 1;276:119363.

Ferwati MS, Ahmad AM, Takalkar GD, Bicer Y. Energy and exergy analysis of parallel flow double effect H2O-[mmim][DMP] absorption refrigeration system for solar powered district cooling. Case Studies in Thermal Engineering. 2021 Dec 1;28:101382.

Varela, R.J., Yamaguchi, S., Giannetti, N., Saito, K., Wang, X.M., Nakayama, H. 2020. Experimental performance analysis and simulation of an internally cooled liquid desiccant air conditioning system using a novel ionic liquid; Refrigeration Science and Technology, 14th IIR Gustav-Lorentzen Conference on Natural Fluids, GL 2020, Virtual, Kyoto, December 2020, Code 165814.

Watanabe H, Komura T, Matsumoto R, Ito K, Nakayama H, Nokami T, Itoh T. Design of ionic liquids as liquid desiccant for an air conditioning system. Green Energy & Environment. 2019 Apr 1;4(2):139-45.

Silaipillayarputhur K, Idem S. A General Matrix Approach to Model Steady-State Performance of Cross-Flow Heat Exchangers. Heat Transfer Engineering. 2013 Jan 1;34(4):338-48.

Zhai C, Sui Z, Wu W. Geometry optimization of plate heat exchangers as absorbers in compact absorption refrigeration systems using H2O/ionic liquids. Applied Thermal Engineering. 2021 Mar 5;186:116554.

Liu X, Li J, Hou K, Wang S, He M. New environment friendly working pairs of dimethyl ether and ionic liquids for absorption refrigeration with high COP. International Journal of Refrigeration. 2022 Feb 1;134:159-67.

de Araújo HV, Massuchetto LH, do Nascimento RB, de Carvalho SM, Dangelo JV. Thermodynamic performance analysis of a single-effect absorption refrigeration system operating with water and 1-ethyl-3-methylimidazolium-based ionic liquids mixtures. Applied Thermal Engineering. 2022 Jan 25;201:117761.

Gao JT, Xu ZY, Wang RZ. Towards high-performance sorption cold energy storage and transmission with ionic liquid absorbents. Energy Conversion and Management. 2021 Aug 1;241:114296.

Li K, Wu W, Peng L, Zhang H. Study on viscosity characteristics of CO2-ionic liquid mixture used for compression-absorption refrigeration systems. Journal of Molecular Liquids. 2021 Sep 1;337:116240.

Zhai C, Sui Y, Sui Z, Wu W. Ionic liquids for microchannel membrane-based absorption heat pumps: Performance comparison and geometry optimization. Energy Conversion and Management. 2021 Jul 1;239:114213.

Ayad A, Di Pietro T, Mutelet F, Negadi A. Thermodynamic Properties of Tricyanomethanide-Based Ionic Liquids with Water: Experimental and Modelling. Journal of Solution Chemistry. 2021 Apr;50(4):517-43.

Theodore L. Bergman, Adrienne S. Lavine, Frank P. Incropera and David P. Dewitt, Fundamentals of Heat and Mass Transfer, Seventh Edition, John Wiley & Sons.

McQuiston, C.F., Parker, D.J., Spitler, D.J., Heating Ventilating and Airconditioning, Sixth Edition, John Wiley & Sons. 2004.
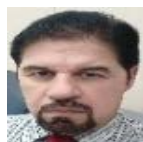
**Dr.Abdulaziz El Sinawi** has been serving King Faisal University since 2007, and he is currently the Chair of Mechanical Engineering Department. He received his PhD from University of Dayton in 2007. His research interests are thermo-fluid systems, energy systems, combustion, etc.

**Dr.Karthik Silaipillayarputhur** has been serving King Faisal University since 2013, and he is with the Department of Mechanical Engineering. He received his PhD from Tennessee Technological University. His research interests are Heat Exchangers, Modeling Heat Transfer Systems, Energy Systems.

**Professor Dr.Christopher Hardacre** is Vice Dean and Head of School of Natural Sciences at the University of Manchester. His research group focuses on Ionic Liquids and Catalysis, with relevant projects in Biomass Processing, energy, fine chemical synthesis, plasma Catalysis for Emission Control and Clean Hydrogen production. Prof. Christopher Hardacre has been appointed the new Director of the UK Catalysis Hub going forward into Phase II.

**Saad Al-Mubarak** finished his undergraduate education in Mechanical Engineering with a high GPA from King Faisal University.

**Mohammed Abdulmohsen Almuhaysh** finished his undergraduate education in Mechanical Engineering with a high GPA from King Faisal University.